A Novel Soft-Switching PWM DC/DC Converter with DC Rail Series Switch-Parallel Capacitor Edge Resonant Snubber Assisted by High-Frequency Transformer Parasitic Components

Khairy Fathy , Hyun Woo Lee and Mutsuo Nakaoka
EESRC, The graduate School of Electrical and Electronics Engineering,
Kyungnam University, Masan, Korea
Khairy_fathy@yahoo.ca

Abstract –. This paper presents two new circuit topologies of DC bus lineside active edge resonant snubber assisted soft-switching PWM full-bridge DC-DC converter acceptable for either utility AC 200V-rms or AC 400V-rms input voltage source. One topology of proposed DC-DC converters is composed of a typical voltage source-fed full-bridge high frequency PWM inverter using DC busline side series power semiconductor switching devices with the aid of a parallel capacitive lossless snubber. All the active power switches in the full-bridge arms and DC busline can achieve ZCS turn-on and ZVS turn-off commutations and the total turn-off switching power losses of all active switches can be reduced for high-frequency switching action. It is proved that the more the switching frequency of full-bridge soft switching inverter increases, the more soft-switching PWM DC-DC converter with a high frequency transformer link has remarkable advantages for its efficiency and power density as compared with the conventional hard-switching PWM inverter type DC-DC converter

I. INTRODUCTION

A. *Research Backgrounds*

Recently, some types of saturable inductor switch assisted phase shift ZVS-PWM full-bridge high-frequency inverter link soft switching DC-DC converters [1] and lossless snubbing capacitors and transformer parasitic inductive components assisted soft-switching DC-DC converter with phase-shift PWM scheme in the secondary-side of high frequency transformer [2]-[5] have been developed and evaluated so far. These DC-DC converter circuit topologies are suitable for handling high output power more than several kW for high/medium voltage and low current applications as new energy related power conditioning supplies. However, secondary side magnetic switches or secondary side semiconductor switch in these high frequency isolated boost transformer link phase shift DC-DC converter circuit topologies may cause large conduction losses in the primary side of transformer when these circuit topologies are adopted for low voltage and large current applications as electro-plating, automotive DC feeding and arc welding power supplies. Therefore, for the low voltage and large current applications, a soft-switching DC-DC converters with active main and auxiliary switches in the primary side of the high frequency transformer is considered to be more suitable and cost effective.

B. *Research Objectives*

Under the practical situation, this paper presents two novel circuit topologies of voltage source full-bridge soft-switching PWM inverters suitable for either utility AC 200V-rms or AC 400V-rms input line, which are composed of typical full-bridge inverter and additional DC busline PWM series switches with the aid of a DC busline parallel lossless capacitive snubber. Under the newly proposed soft-switching PWM full-bridge DC-DC converters with high frequency transformer, all the active switches in the full-bridge arms and DC busline can actively achieve ZVS/ZVT turn-off commutation operation. The operating principles of the soft-switching PWM full-bridge DC-DC converters tested here are described, along with its remarkable features. The experimental operation results of these types of soft-switching PWM full-bridge DC-DC converters using IGBT power modules are illustrated including power loss analysis as compared with those of hard-switching PWM DC-DC converter

II. DC-DC Converter for Utility AC 200V-rms

A. *Circuit Description*

Fig. 1 shows a novel high frequency transformer linked soft-switching PWM DC-DC converter acceptable for utility AC 200V-rms. This converter is composed of voltage source full-bridge inverter with active switches in series with DC busline and a single lossless snubbing capacitor in parallel with DC busline, a high frequency transformer with secondary side center-taped windings, DC reactor filter and DC load as arc welder and electroplater. In the newly-developed DC-DC converter, the active edge resonant PWM switches; reverse conducting IGBT $Q_5(S_5/D_5)$ and $Q_6(S_6/D_6)$ in series with DC busline and a lossless capacitor in paralleled with DC busline are added in series with the DC power busline connected to the voltage source full-bridge high frequency inverter composed of the bridge arm switches $Q_1(S_1/D_1)$, $Q_2(S_2/D_2)$, $Q_3(S_3/D_3)$ and $Q_4(S_4/D_4)$. In particular, it is noted that a single small lossless snubbing capacitor C in DC input busline is inserted between active switches Q_5, Q_6 and the full-bridge type inverter in order to achieve ZVS.

B. *Gate Pulse Timing Sequences*

Fig. 2 depicts pattern-timing sequences of the switching gate driving pulses to be provided to the semiconductor switching devices; IGBTs;Q_1-Q_4, Q_5, Q_6.

The gate voltage pulse signals with a certain dead time, which are delivered to Q_1 and Q_4 or Q_2 and Q_3 in the diagonal bridge arms of the voltage source full-bridge inverter arms, are the same as signal sequences of conventional full-bridge inverter. Regarding the turn-on gate pulse voltage signals to the DC busline side series switches Q_5 and Q_6, the gate signals are applied to Q_5 or Q_6 at the same timing pulse period as the turn-on gate pulse signals to Q_1 and Q_4 or Q_2 and Q_3, respectively. As for the turn-off gate pulse voltage signals to Q_5 or Q_6, the gate pulses are delivered to Q_5 or Q_6 before the predetermined specific length of time t_d on the basis of the time when the turn-off signals are respectively applied to the switches Q_1 and Q_4 or Q_2 and Q_3.

C. Operation Principle of Converter Topology I

Fig. 3 illustrates the relevant voltage operating waveforms the DC-DC converter circuit for utility AC 200V-rms input in a complete switching period specified by the pulse pattern of gate drive timing sequences shown in Fig. 2. The operation modes of the converter circuit for the utility AC 200V-rms input are divided into seven operation modes from mode 0 to mode 6 in accordance with operation timing transitions from t_0 to t_6 and its operation principle is described in the following. The equivalent circuits corresponding to each mode are shown in Fig.4.

1) Mode 0: -t_0

Before time t_0, the switches Q_1, Q_4 and Q_5 are turned on simultaneously. During this time, the primary side energy is supplied to the load R in the secondary circuit through the high frequency transformer HF-T.

2) Mode 1:t_0-t_1

At time $t = t_0$, the series switch Q_5 in DC busline side is turned off. At this time, the series switch Q_5 can turn off with ZVS because the current i_{S5} through Q_5 is immediately cut off with the aid of the lossless snubbing capacitor C. The supply DC voltage source is cut off from the DC-DC converter with a high frequency transformer. After time t_0, the voltage v_C across the lossless snubbing capacitor C decreases toward zero from E. During this period, the voltage v_C across the lossless snubber capacitor C can be approximately estimated as,

$$v_c(t) = E - (i_{l1} / C)\, t \qquad (1)$$

where, i_{l1} is a primary current of high frequency transformer with voltage step down turns ratio. From eq. (1), the discharging time t_{dc} of the capacitor C until the voltage v_C becomes zero is given by,

$$t_{dc} = CE / i_{l1} \qquad (2)$$

Under this newly-developed DC-DC converter circuit, an appropriate delay time t_d indicated in Fig. 2 is designed so as to be a little longer than the time calculated from eq. (2) under the condition of the maximum i_{l1} or the maximum output current. In this case, the switches Q_1 and Q_4 or Q_2 and Q_3 can achieve ZVS transition completely. If we need to widen the complete ZVS operation range at the turn-off commutation for the switches Q_1 and Q_4 or Q_2 and Q_3, the optimum delay time t_d should be varied according to the value of the maximum current i_{l1} of high frequency transformer.

3) Mode 2:t_1-t_2

At time $t = t_1$, the voltage v_C is completely decreases to zero. In the interval from t_1 to t_2, the diodes D_2 of Q_2 and D_3 of Q_3 are turned on. The current i_{l1} through the high frequency transformer primary winding flows through two closed loops; $L_S \rightarrow D_3 \rightarrow S_1 \rightarrow L_S$ and $L_S \rightarrow S_4 \rightarrow D_2 \rightarrow L_S$.

4) Mode 3:t_2-t_3

At time $t = t_2$, the switches Q_1 and Q_4 are turned-off. At this time, because the voltage v_C across the lossless snubbing quasi-resonant capacitor has been already equal to zero. The diodes D_2 of Q_2 and D_3 of Q_3 immediately turn on, the active switches Q_1 and Q_4 can be turned off with ZVS.At this mode, the condition that the lossless snubber capacitor C in parallel with DC busline has been just charged up to the same voltage as DC busline voltage E can be estimated by eq. (3).

$$(1/2)CE^2 = (1/2)\, L_S\, (i_{l1})^2 \qquad (3)$$

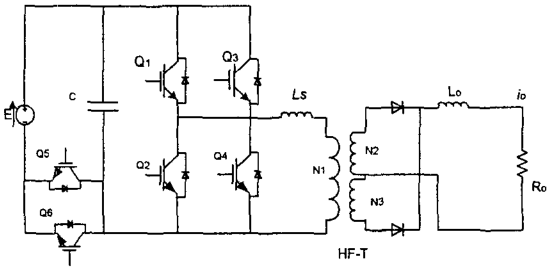

Fig. 1 Soft-switching PWM DC-DC power converter with high frequency transformer link for utility AC 200V-rms input

However, as described after, in mode 6, the circuit parameters should be designed to meet the condition of $(1/2)CE^2 < (1/2)L_S(i_{l1})^2$ in order to achieve ZVS commutation at turn-on transition of the switch Q_6.

5) Mode 4:t_3-t_4

Under a condition of $(1/2)CE^2 < (1/2)L_S(i_{l1})^2$, the voltage v_C across the snubber capacitor C is clamped to DC busline voltage E after the voltage v_C reaches the DC busline voltage E, because the diodes D_5 of Q_5 and D_6 of Q_6 are turned on and the energy stored into leakage inductance L_S of high frequency transformer is returned back to the DC busline voltage source E.

6) Mode 5:t_4-t_5

In this mode, all the operations are stopped in the primary circuit of high frequency transformer, except the voltages across the switches Q_1 and Q_4 decrease down to $(1/2)E$ and the voltages across the switches Q_2 and Q_3 increase up to $(1/2)E$ due to parasitic parameters of the switches Q_1,Q_2, Q_3 and Q_4.

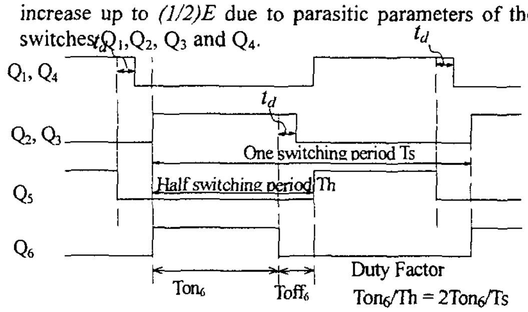

Fig. 2 Pattern sequences of switching gate driving pulses

7) Mode 6:t_5-t_6

At time $t = t_5$, the switches Q_2, Q_3 and Q_6 are turned on respectively. At this time, the switches Q_2, Q_3 can be turned on with ZCS because of parasitic inductance L_S of the high frequency transformer. And more, the switch Q_6 can achieves ZVS/ZCS at a turn-on transition commutation because the voltage v_C is the same as DC power busline voltage.

Thereafter, the aforementioned operating processes are repeated in sequence during each switching cycle

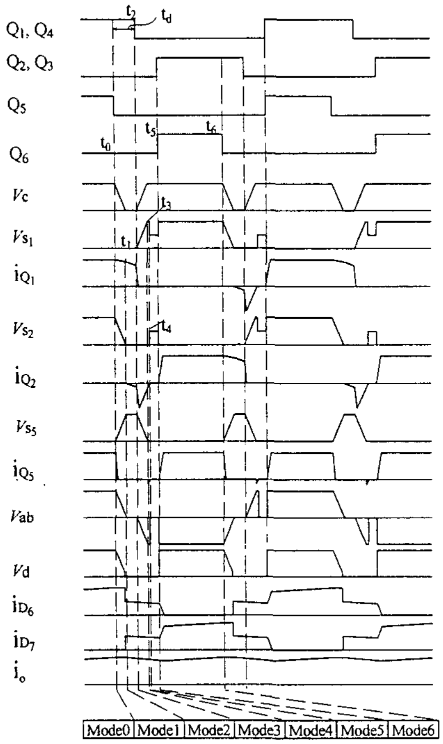

Fig. 3 Operating waveforms of the circuit for AC 200V-rms input during one switching period

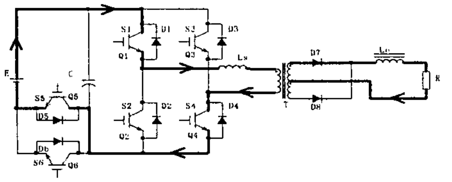

(a) Mode 0 ($-t_0$); Energy transfer to secondary during turn-on of Q_1,Q_4 and Q_5

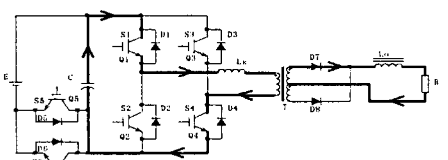

(b) Mode 1 (t_0-t_1); Discharge of C after Q_5 being turned off

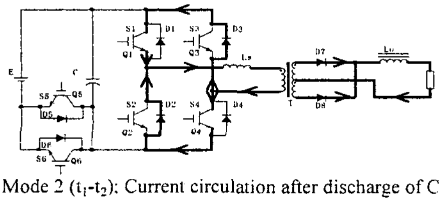

(c) Mode 2 (t_1-t_2); Current circulation after discharge of C

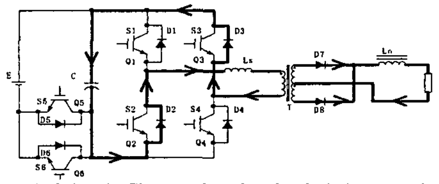

(d) Mode 3 (t_2-t_3); Charge of C after Q_1, Q_4 being turned off

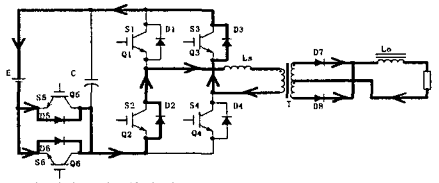

(e) Mode 4 (t_3-t_4); Vc being clamped by E

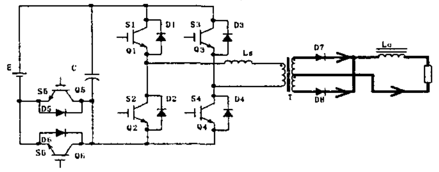

(f) Mode 5 (t_4-t_5); No operation in primary circuit

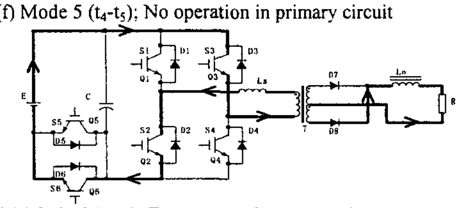

(g) Mode 6 (t_5-t_6); Energy transfer to secondary during turn-on of Q_2,Q_3 and Q_6

Fig. 4 Equivalent circuits for seven switching operation modes

III. New Soft Switching PWM DC-DC Converter for Utility AC 400V-rms Grid

A. Circuit Description of Converter Topology II

Fig. 5 shows a planner type high frequency transformer linked soft-switching PWM DC-DC converter topology acceptable for utility AC 400V-rms input. Under the DC-DC converter used for utility AC 400V input, the DC busline voltage source is selectively operated by divided voltage sources E_1 and E_2. The voltages E_1 and E_2 ($E_1 = E_2$) are designed so as to be equal to E. The switch Q_5 in Fig. 1 is moved to the high side of DC busline in Fig. 5. The diodes D_9 and D_{10} in series are also inserted in parallel with the DC busline between Q_5 or Q_6 and full-bridge inverter arms. And the center point between E_1 and E_2 is directly connected to the mid point between the diodes D_9 and D_{10}.

B. Gate Pulse Timing Sequences and Operating Principle

The timing pattern sequences of switching gate driving pulses for the utility AC 400V-rms input grid are exactly the same as that for the utility AC200V-rms input shown in Fig. 2. Under the newly-developed DC-DC converter topology II suitable for the utility AC 400V-rms input, when the switches Q_5 or Q_6 are turned on and off alternately, half voltage E of DC busline voltage $2E$

(E_1=E_2=E) is applied to the lossless snubbing capacitor C in parallel with DC busline and full-bridge inverter arms. Therefore, the same IGBTs rating as IGBTs in the converter circuit topology I for utility AC 200V-rms input can be used even in the circuit for the utility AC 400V-rms input grid.

In addition to this feature, when the switches Q_1, Q_4 and Q_5 or Q_2, Q_3 and Q_6 are turned on and turned off alternately at the same timing pulses as those for the switches in the DC-DC converter topology I employed for the utility AC 200V-rms input shown in Fig. 1, all the switches can perform ZVS turn-off and perform ZCS or ZVS/ZCS turn-on transitions as all the switches in the DC-DC converter circuit topology I used for the utility AC 200V-rms input grid. The operating waveforms of the converter circuit topology II for the AC 400V-rms input grid are almost the same as that of the converter circuit topology I for the AC 200V-rms input grid. The main diference between circuit operation with AC 200V and circuit operation with AC 400V is that the voltage v_C across the capacitor C is not clamped to DC busline voltage in case of the circuit for AC 400V-rms input.

IV. Experimental Results and Discussions

A. System Implementations for 200V and 400V Utility AC grids

The experimental setups for the soft-switching PWM DC-DC power converter circuits I and II with high frequency transformers applied for either the utility AC 200V-rms or AC 400V-rms dual inputs are implemented in Fig. 6 and Fig. 7, respectively.

In Table1, the design specifications and circuit parameters are listed for two converters I, II respectively. Under the both DC-DC power converter circuits shown in Fig. 6 and Fig. 7, the 2in1 IGBT power modules 2MBI150TA-060(I_C=150A, V_{CES}=600V) produced by Fuji Electric Co. Ltd are used for all the active power switches. In Fig. 6, each IGBT with reverse conducting diode in the 2in1 IGBT power modules is used for the DC busline series switches $Q_5(S_5/D_5)$ and $Q_6(S_6/D_6)$ and another IGBT with reverse conducting diode in the 2in1 IGBT power modules is not in use. In Fig. 7, each IGBT with reverse conducting diode and one reverse conducting diode in the 2in1 IGBT power modules are used for the active PWM switches $Q_5(S_5/D_5)$, D_9 and $Q_6(S_6/D_6)$, D_{10} , all the switches and circuit components used in Fig. 5 and Fig. 6 are completely the same constants and ratings. Fig. 7 demonstrates the whole appearance of the experimental setup using CO_2/MAG arc welding power supply for both utility AC 200V-rms and AC 400V-rms input. The maximum output rating of this experimental setup is 36V, 350A (12.6kW).

Fig. 8 represents the assembled component appearance in the transformer primary side of the main power converter circuit used in the experimental setup in Fig. 5

The only difference on the assembled components in the transformer primary side of the main DC-DC power converter circuit topologies I, II between the experimental setups in Fig. 6 and in Fig. 7 should be the printed circuit board designed for the circuit wiring connections. The IGBT modules are mounted on the heat sink and connected by the printed circuit board on which the capacitors C_1, C_2 and C_3=C are mounted. The switches; IGBTs, the capacitors C_1, C_2 and C_3=C on the printed circuit board enables to minimize the stray inductance at wiring connections among IGBTs, C_1, C_2 and C_3=C. Actually, the minimum leakage inductance assembled by the printed circuit board connections is particularly an important factor on this newly-developed soft-switching PWM DC-DC power converter I, II, because spike voltage across collector and emitter of IGBTs is easy to appears at a turn off dynamic transition if there is wiring stray inductances between the snubbing capacitor C_3=C and the IGBT switches in full-bridge inverter arms and DC busline.

B. Measured Switching Voltage and Current Waveforms

In experimental implementation, the switching operating voltage and current waveforms under maximum output power (36V, 350A) for utility AC 400V-rms input when the switch Q_1 is turned on and turned off are depicted in Fig. 8 (a) and (b), respectively.

Observing these switching waveforms in Fig. 10, the switch Q_1 is turned on with ZCS and turned off with ZVS. The switching voltage and current waveforms under the maximum output power ratings (36V, 350A) are respectively shown in Fig. 8 (c) and (d) when the switch Q_5 is turned on and turned off.

Observing the operating switching waveforms, the switch Q_5 is completely turned on with ZVS/ZCS and is turned off with ZVS. However, at the turn-off mode transition processing for switches falling current and Q_1 and Q_5, some power losses still exists due to inherent tail current characteristics of the used IGBTs.

C. Power Loss Analysis

Considering power loss analysis in Fig. 8, the total power losses of all the active switches in the full-bridge arms including Q_5 and Q_6 in DC busline for the newly-developed soft-switching PWM DC-DC power converter circuits I, II for utility AC 200V-rms and AC 400V-rms input shown in Fig. 5 and Fig. 6 are compared with those of all the switches in conventional hard-switching PWM inverter type DC-DC converters with a high frequency DC link. When the switching frequency is about 20 kHz, the total power losses for soft-switching PWM DC-DC inverter type power converter and hard-switching PWM inverter type DC-DC converter are almost equal. The switching frequency of voltage source full-bridge high frequency inverter power stage using IGBTs is designed so as to be more than about 20 kHz. The more the switching frequency of full-bridge high frequency inverter increases, the more two newly-developed DC-DC power converter circuits I, II can have remarkable advantages from the points view of the power conversion efficiency and power density as compared with those of the conventional hard-switching inverter type DC-DC power converter.

In case the switching frequency is designed for 40 kHz or the ripple frequency 80 kHz, the total power losses for all the switches in newly-developed soft-switching PWM DC-DC power converter circuits I, II with a high frequency inverter are 405 W in case of AC 200V-rms input and 465 W in case of AC 400V-rms input, respectively. On the other hand, those of the conventional hard-switching PWM inverter type DC-DC converters are 510 W and 600 W, respectively. Furthermore, the typical RC snubber circuits are necessarily for the conventional high frequency transformer link hard-switching PWM DC-DC power converter. Therefore, the total power losses for conventional high frequency transformer link hard-switching PWM DC-DC power converter including the power loss of RC snubber circuits are estimated as about 785 W in case of utility AC 200V-rms input and 1100 W in case of utility AC 400V-rms input, respectively. These power losses are about two times more than the total power loss of newly-developed converter circuit I in case of AC 200V-rms input and two times more than that of newly-developed converter circuit II in case of AC 400V-rms input.

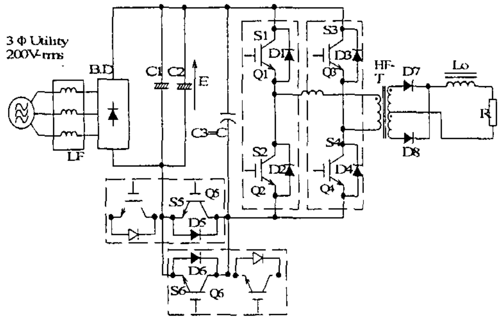

Fig. 5 Experimental setup for utility AC 200V-rms input grid

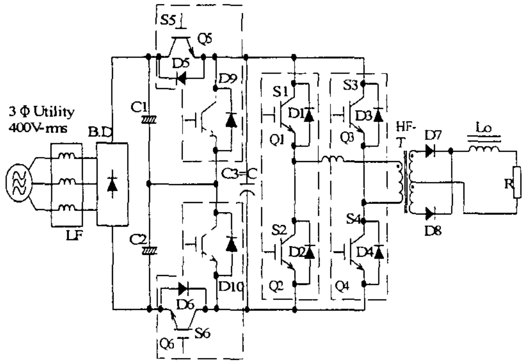

Fig. 6 Experimental setup for utility AC 200V-rms input grid

Fig. 7 Whole appearance of experimental setup of CO2/MAG arc welding power supply for dual input of utility AC 200V-rms and AC 400V-rms input

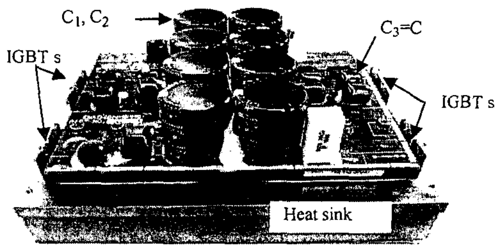

Fig. 8 Assembled component appearance in transformer primary side circuit of soft-switching PWM DC-DC power converter

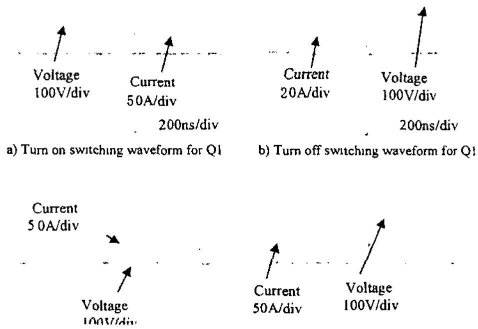

Fig. 9 Measured switching voltage and current waveforms for the switches Q_1, Q_5 under the circuit for 5
utility AC 400V-rms input

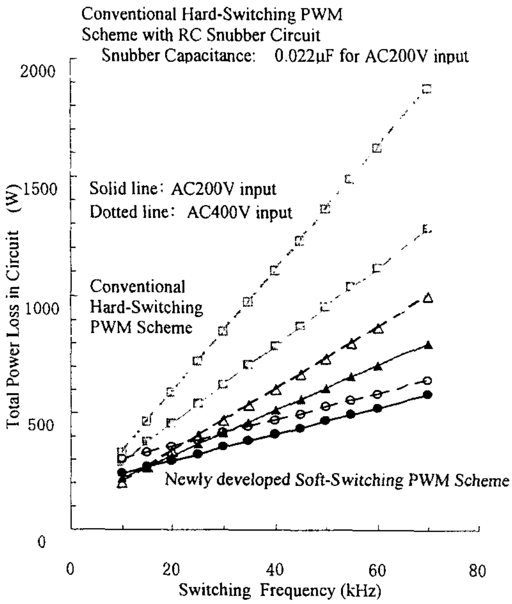

Fig. 10 Comparative power loss analysis between newly-developed soft-switching PWM and conventional hard-switching PWM DC-DC power converters

D. Arc Welding Products

Under the experimental setup implementation of CO_2/MAG arc welding power supply equipment shown in Fig. 8 using the proposed power converter, the volumetric size is 59% less and its weight is 47% less than these of conventional CO_2/MAG arc welding power supply equipment using hard-switching PWM inverter using IGBT power modules, because the newly-developed high frequency transformer link soft-switching PWM full-bridge DC-DC power converter circuit I, II enables 40 kHz switching frequency for the new generation CO_2/MAG arc welding power supply equipment without increasing the power loss of the active power switches, while the inverter switching frequency of conventional arc welding power supply equipment is designed so as to be 13 kHz for hard-switching PWM operation. In addition to this, the arc welding dynamic performance can be much improved by fast control responses in accordance with the high switching frequency.

V. CONCLUSIONS

In this paper, two new circuit topologies of soft-switching PWM DC-DC power converters I, II with planner type high frequency transformer suitable and acceptable for the utility AC 200V-rms or 400V-rms selective dual voltage input specifications have been presented, which are composed of the voltage source-fed full-bridge inverter with additional series PWM switches in DC busline and a parallel lossless capacitive snubber between DC busline ports, a planner type high frequency transformer with its secondary side winding center tapped configuration, or a full-wave diode rectifier and a DC reactor in series with the load for low voltage large current specifications.

The power loss analysis of soft-switching PWM DC-DC power converters with a high frequency transformer link have been discussed and evaluated as compared with that of hard-switching PWM DC-DC power converter with a high frequency transformer link. The practical effectiveness of the proposed two DC-DC power converter topologies operating under a principle of soft-switching PWM scheme have been actually proved from a practical point of view for the utility AC 200V and the AC 400V and the high efficiency and high power density of two types of DC-DC power converters could be achieved on the basis of the experimental results for the latest CO2/MAG arc welder put into practice.

The main features of two prototypes of newly-developed soft-switching PWM DC-DC power converters with a planner type high frequency transformer can be summarized as follows;

(1) By adding a simple circuit configuration of additional semiconductor switching devices connected in series with DC rail and a passive paralleled power capacitor component to the conventional full-bridge hard-switching PWM inverter, all the active semiconductor switching devices can achieve ZVS turn-off commutation and ZCS turn-on soft commutation. Therefore, although the total conduction power losses of the additional switches and capacitor snubber increase a little, the total turn-off switching loss of the voltage source full-bridge type PWM inverters can be significantly decreased when the switching frequency of high frequency inverter power stages using IGBTs is selected more than about 20 kHz.

(2) The newly-developed DC-DC power converter circuits I, II can be used for the both utility AC 200V-rms and AC 400V-rms dual voltage input line without replacing any semiconductor switching devices and high frequency transformer by means of changing lead wiring connections only. Thus, the newly-developed soft-switching PWM DC-DC power converter circuits I, II with a planner type high frequency transformer has a cost effective applicability for the utility AC 200V/400V input voltages.

(3) The control circuit for newly-developed circuits can be implemented easily by modifying the conventional PWM signal processing circuit using common PWM control IC(μPC494).

ACKNOWLEDGMENT

This work was financially supported by MOCIE through IERC program

REFERENCES

[1] S. Hamada, M. Nakaoka, "Saturable Inductor-Assisted ZVS-PWM Full-Bridge High-Frequency Link DC-DC Power Converter Operating and Conduction Losses", Proceedings of IEE-UK International Conference on Power Electronics and Variable-Speed Drives, pp.483-488, October, 1994.

[2] O. D .Patterson and D. M. Divan, "Pseudo-Resonant Full Bridge DC/DC Converter", Records of IEEE-PESC, pp.424-430, June,1987.

[3] M. Michihira, M. Nakaoka, "A Novel Quasi-Resonant DC-DC Converter using Phase-Shifted Modulation in Secondary-Side of High-Frequency Transformer", Records of IEEE-PELS Power Electronics Specialists Conference, Vol.1, pp100-105, June, 1996.

[4] M. Michihira, T. Funaki, M. Nakaoka, K. Matsu-ura, "A Novel quasi-resonant DC-DC converter using phase-shift PWM control at secondary side of high-frequency transformer", Proceedings of Japan Society Power Electronics , Vol.21, No2, pp78-87, 1996.

[5] S. Moisseev, S. Hamada, M. Nakaoka, "Novel Soft-Switching Phase-Shift PWM DC-DC Converter", Proceedings of Japan Society Power Electronics , Vol.28, pp107-116, 2003.

[6] K. Morimoto, T. Doi, H. Manabe, M. Nakaoka, H.W. Lee, "Advanced High Power DC-DC Converter using Novel Type Full-Bridge Soft-Switching PWM Inverter with High Frequency Transformer Link for Arc Welding Application". Proceedings of KIPE-ICPE, pp. II 191- II 197, October, 2004.

[7] K. Morimoto, T. Doi, H. Manabe, M. Nakaoka, N.A. Ahmed, H.W. Lee, E. Hiraki, T. Ahmed, "Next Generation High Efficiency High Power DC-DC Converter incorporating Active Switch and Snubbing Capacitor Assisted Full-Bridge Soft-Switching PWM Inverter with High Frequency Transformer for Large Current Output", Proceedings of IEEE-APEC, pp1549-1555, March, 2005

[8] K. Morimoto, T. Doi, H. Manabe, N.A. Ahmed, H.W. Lee, M. Nakaoka, T. Ahmed, "A Novel High-Frequency Transformer Linked Soft-Switching Pulse Modulation DC-DC Power Supply for Arc Welder", Proceedings of PCIM China , pp 43-48, March, 2005